proceedings

MDPI

Proceedings

Alkynyl *N*-BODIPYs as Reactive Intermediates for the Development of Dyes for Biophotonics †

César Ray [1], Andrés García-Sampedro [2], Christopher Schad [1], Edurne Avellanal-Zaballa [3], Florencio Moreno [1], María J. Ortiz [1], Jorge Bañuelos [3], Angeles Villanueva [4,5], Pilar Acedo [2], Beatriz L. Maroto [1,*] and Santiago de la Moya [1,*]

[1] Departamento de Química Orgánica, Facultad de Ciencias Químicas, Universidad Complutense de Madrid, Ciudad Universitaria s/n, 28040 Madrid, Spain; cesarrayleiva@ucm.es (C.R.); cschad@ucm.es (C.S.); floren@ucm.es (F.M.); mjortiz@quim.ucm.es (M.J.O.)

[2] Institute for Liver and Digestive Health, University College London, Pond Street, London NW3 2PG, UK; andres.sampedro.17@ucl.ac.uk (A.G.-S.); p.nunez@ucl.ac.uk (P.A.)

[3] Departamento de Química Física, Facultad de Ciencia y Tecnología, Universidad del País Vasco-EHU, 48080 Bilbao, Spain; edurne.avellanal@ehu.eus (E.A.-Z.); jorge.banuelos@ehu.eus (J.B.)

[4] Departamento de Biología, Universidad Autónoma de Madrid, Darwin 2, 28049 Madrid, Spain; angeles.villanueva@uam.es

[5] Instituto Madrileño de Estudios Avanzados (IMDEA) Nanociencia, Ciudad Universitaria de Cantoblanco, 28049 Madrid, Spain

* Correspondence:Correspondence: belora@ucm.es (B.L.M.); santmoya@ucm.es (S.d.l.M.); Tel.: +34-913944716 (B.L.M.); +34-913945090 (S.d.l.M.)

† Presented at the 24th International Electronic Conference on Synthetic Organic Chemistry, 15 November–15 December 2020; Available online: https://ecsoc-24.sciforum.net/.

Published: date

Abstract: A new approach for the rapid multi-functionalization of BODIPY dyes towards biophotonics is reported. It is based on novel *N*-BODIPYs, through reactive intermediates with alkynyl groups to be further derivatized by *click chemistry*. This approach has been exemplified by the development of new dyes for cell bio-imaging, which have proven to successfully internalize into pancreatic cancer cells and accumulate in the mitochondria. The in vitro suitability for photodynamic therapy (PDT) was also analyzed and confirmed our compounds to be promising PDT candidates for the treatment of pancreatic cancer.

Keywords: *N*-BODIPYs; biophotonics; BODIPY functionalization; PDT; pancreatic cancer

1. Introduction

Biophotonics, which is the application of photonics to life science [1], is a rapidly growing multidisciplinary field that includes monitoring of cellular processes, optical diagnostics and light-activated treatments, like photodynamic therapy (PDT) [2–6]. The advancement in biophotonics requires the development of efficient photonic systems that can act as bioprobes or PDT agents or, what is more interesting, that can integrate imaging and therapy into a single platform. This last approach, named as theranostics, is considered one of the most promising precision medicine technologies in cancer [7]. However, the development of photonic systems that can be efficiently applied to biophotonics is not an easy task since many requisites need to be fulfilled within the same system: good photonic properties (high fluorescence or/and singlet oxygen generation, photostability), specificity (cell permeability and organelle recognition), biocompatibility (solubility, low dark toxicity), etc. In this context, monochromophoric organic dyes have advantages related to

accessibility and biocompatibility and, especially, the possibility of modulating key properties by chemical modifications [8–11].

Among all the organic dyes, BODIPYs (Boron DIPYrromethenes, Figure 1) are worth highlighting due to their excellent photophysical properties, which can be adjusted by appropriate chemical modifications of the chromophore structure [12–15]. To apply them in biophotonics, it is necessary to introduce additional functional groups for bio-recognition [16] or for increasing water solubility [17], likely the main drawback of BODIPYs. Unfortunately, this is not an easy step in monochromophoric BODIPYs, because the introduction of additional functional groups can severely affect the optimized photophysical properties of the chromophore. In this sense, among all the possible positions in BODIPY, functionalization at boron is a privileged position because the boron atom is not part of the chromophore [18] and, therefore, functionalization at boron should be the preferred option to endow BODIPY dyes with key properties, without affecting the ground photophysical properties of the involved chromophore.

In this context, we have recently reported the straightforward preparation of *N*-BODIPYs, this is, BODIPYs having *N*-groups at boron (Figure 1) [19]. While keeping the photophysical properties of parent *F*-BODIPYs (see Figure 1), *N*-BODIPYs have the advantage, over other related at-boron-functionalized BODIPYs, such as *O*-BODIPYs, that up to four different moieties can be placed near the BODIPY chromophore, due to the bonding features of the nitrogen atom in comparison with oxygen. Thus, the *N*-BODIPY design is an attractive scaffold to engineer smart BODIPYs with multiple functions, which is especially interesting when developing BODIPYs for biophotonics.

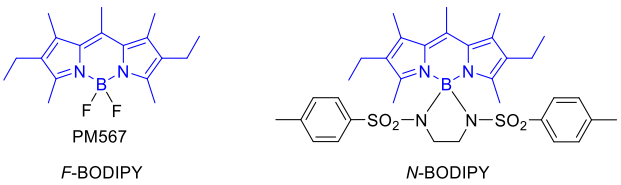

Figure 1. Examples of *F*- and *N*-BODIPYs.

A strategy that is being widely used nowadays for the functionalization of dyes directed towards biophotonics is the use of *click chemistry* between alkyne- and azide-functionalized building blocks. The most interesting feature of this reaction for biophotonics is that it can be carried out *in vivo*, even inside of the human body. This fact has advantages related to avoiding the toxicity of some molecules (the probe or drug is generated at a specific site in the body), facilitating permeation of the acting molecule (the molecule enters the cell divided into pieces and it is build inside the cell), etc. [20].

2. Results and Discussion

2.1. Design and Synthesis

2.1.1. Synthesis of the Alkyne-Based Key Intermediate

Following our initial hypothesis, we designed *N*-BODIPY **NBPD-yne** as a key intermediate to BODIPY dyes for cell-imaging, based on the following premises: (1) functionalization at boron to keep the excellent photophysical signature of parent *F*-BODIPY; (2) straightforward synthesis from commercially available *F*-BODIPY; (3) possibility of multifunctionalization through the *N*-groups; (4) alkynyl group for the easy post-derivatization (by *click-chemistry*) for bio-recognition.

We successfully applied the methodology developed by us for the synthesis of *N*-BODIPYs [19] to the synthesis of **NBDP-yne** from parent *F*-BODIPY (2,6-diethyl-1,3,5,7,8-pentamethyl-*F*-BODIPY, PM567) and the corresponding bis-sulfonamide **2** (see Scheme 1). The procedure is based on the substitution of PM567 fluorine atoms with the bis-sulfonamide nitrogens, activated by boron trichloride at room temperature. In turn, **2** was obtained from commercially available reagents in three easy steps: a double sulfonamidation by reaction of excess of ethane-1,2-diamine with butanesulfonyl chloride, followed by reaction with chlorosulfonylbenzoic acid; and a final esterification

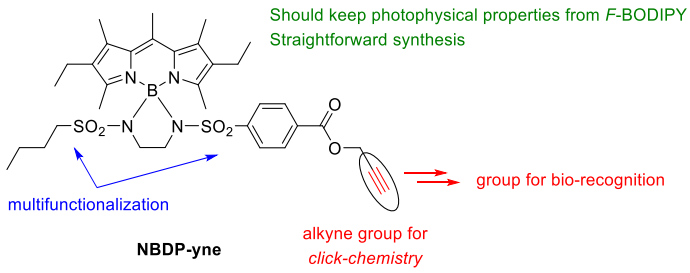

Figure 2. *N*-BODIPY **NBDP-yne** designed as a key intermediate to BODIPY dyes for biophotonics.

With propargyl alcohol, activated with carbodiimide, to yield **2**. Thus, bis-sulfonamide **2** is properly functionalized with an alkyne moiety for further *click-chemistry* and a butane chain to aid in solubility for further chemical manipulations (Scheme 1).

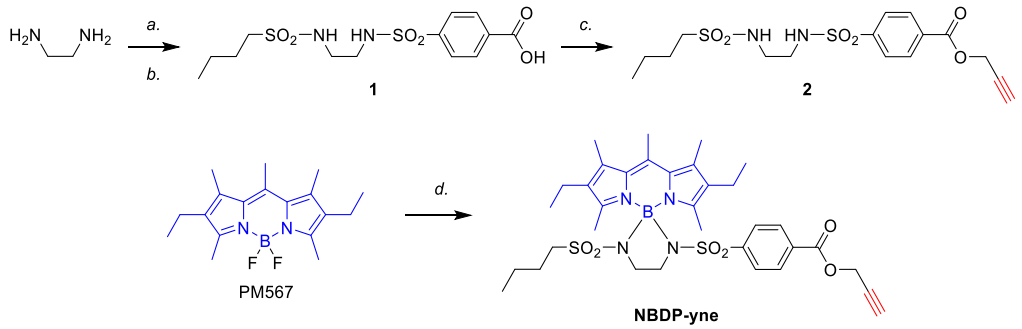

Scheme 1. Synthesis of **NBDP-yne** from parent *F*-BODIPY. *a*. *n*-BuSO$_2$Cl, CH$_2$Cl$_2$, rt, 86%; *b*. 4-(chlorosulfonyl)benzoic acid, NEt$_3$, CH$_2$Cl$_2$, rt, 95%; *c*. propargyl alcohol, EDC·HCl, DMAP, CH$_2$Cl$_2$, rt, 95%; *d*. (i) BCl$_3$, CH$_2$Cl$_2$, rt, (ii) NEt$_3$, (iii) **2**, 72%. DMAP: 4-(dimethylamino)pyridine; EDC: *N*-[3-(dimethylamino)propyl]-*N*′-ethylcarbodiimide.

2.1.2. Derivatization of Key Intermediate NBDP-Yne Towards Bio-Recognition

Once we had intermediate **NBDP-yne** in hand, we proceeded to its chemical derivatization. As a proof of concept, we chose to introduce ammonium and phosphonium moieties as groups that had been described before for the labelling of mitochondria [21–24]. These groups where easily introduced by standard *click-chemistry* (CuSO$_4$, sodium ascorbate) in **NBDP-yne**, using the corresponding azide-functionalized reagent (see Scheme 2).

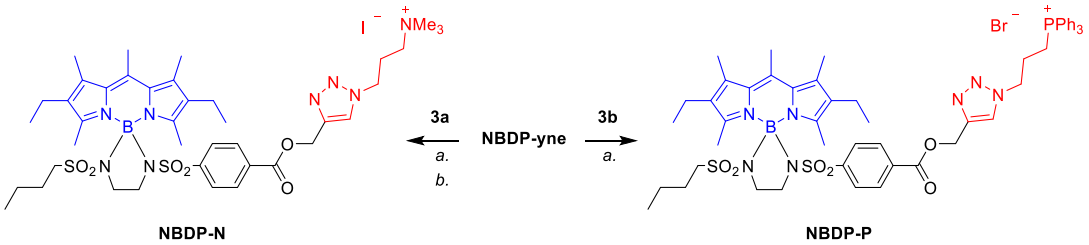

Scheme 2. Postfunctionalization of key intermediate **NBDP-yne** by *click chemistry* with ammonium or phosphonium groups for bio-recognition by mitochondria. *a*. **3a** or **3b**, CuCO$_4$, sodium ascorbate, EtOH, H$_2$O, rt. *b*. MeI, CHCl$_3$, rt. 95% for **NBDP-N**; 84% for **NBDP-P**. **3a**: 3-azido-*N*,*N*-dimethylpropanamine; **3b**: (3-azidopropyl)triphenylphosphonium bromide.

2.2. Spectroscopic Signatures in Solution

As aforementioned in the introduction, the chemical modification at the boron atom is a suitable approach to functionalize the BODIPY with low impact into their photophysical signatures. Following this line of reasoning, the spectral band position of the herein reported three *N*-BODIPYs

is almost the same, regardless of the pendant chain in the sulfonamide of the spiranic ring (see Figure 3). Furthermore, such bands are hardly affected by the environmental properties, a typical feature of BODIPYs [12]. The intermediate *N*-BODIPY (**NBDP-yne**), with the key alkynyl unit, displays a high fluorescence response with efficiencies surpassing 80%, in agreement with the reported results for this new family of BODIPYs [19]. In this regard, the conformational restriction afforded by the spiranic ring sharing the boron center is a key issue to avoid undesirable non-radiative deactivation channels related to internal conversion. Consequently, even the cationic *N*-BODIPYs (**NBDP-N** and **-P**) retain a similar fluorescence efficiency after further functionalization to enable biorecognition, regardless of the introduced functional group (ammonium or phosphonium; Figure 3). In other words, even after chemical modification of the intermediate *N*-BODIPY towards biorecognition, the notable photophysical properties of parent *F*-BODIPYs are kept. That is to say, high absorption coefficient to absorb efficiently the incoming excitation light under the fluorescence microscope, and stable and glow emission for an easy monitorization of the fluorescent imaging after internalization into the cell and labelling of mitochondria. Therefore, both **NBDP-N** and **-P** meet *a priori* all the desired requirements to provide bright and long-lasting fluorescent images in the cellular media to track mitochondria.

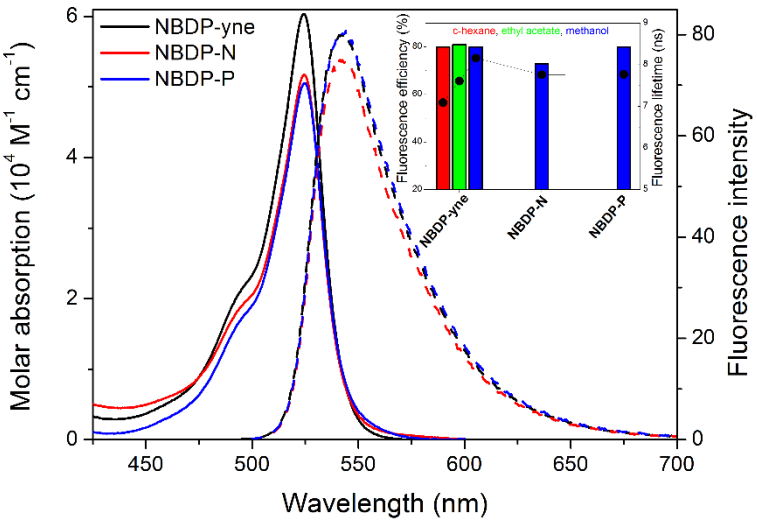

Figure 3. Absorption (scaled by the molar absorption coefficients) and fluorescence (dashed, scaled by the fluorescence quantum yield) spectra of the three designed *N*-BODIPYs (**NBDP-yne, -N** and **-P)** in diluted solutions in methanol (micromolar). Inset: corresponding fluorescence quantum yield and lifetime data.

2.3. Biological Assessment in Established Pancreatic Adenocarcinoma Cells

2.3.1. Photodynamic Therapy Protocols

The suitability of the *N*-BODIPYs **NBDP-P** and **NBDP-N** for PDT treatment of pancreatic cancer was tested (Figure 4A,B). Incubation with increasing concentrations of *N*-BODIPYs followed by irradiation showed that concentrations equal or superior to 10 μM of **NBDP-P** and 25 μM of **NBDP-N** decreased the surviving fraction of cells compared with non-irradiated cells (dark conditions). Both compounds efficiently killed PANC-1 cells, showing an IC50 concentration of 15 μM for **NBDP-P** and 40 μM for **NBDP-N**, positioning these two compounds as promising platforms for the development of photodynamic cancer therapy agents.

2.3.2. N-BODIPYs Internalization in PANC-1 Cells

Incubation of PANC-1 cells with both *N*-BODIPYs (**NBDP-P** and **NBDP-N**) and posterior analysis by flow cytometry revealed that both compounds efficiently internalized in the cells. Incubation with the compounds for 3 or 24 h showed that the cellular uptake occurred rapidly since

the average of fluorescence quantified in the cells was similar for both incubation times (Figure 4C,D). Cells not incubated with *N*-BODIPYs (untreated control group, red histogram in Figure 4C,D) were used to establish the baseline fluorescence signal, which was subtracted from the rest of the samples to determine the positive population of cells exhibiting fluorescence derived from the compounds.

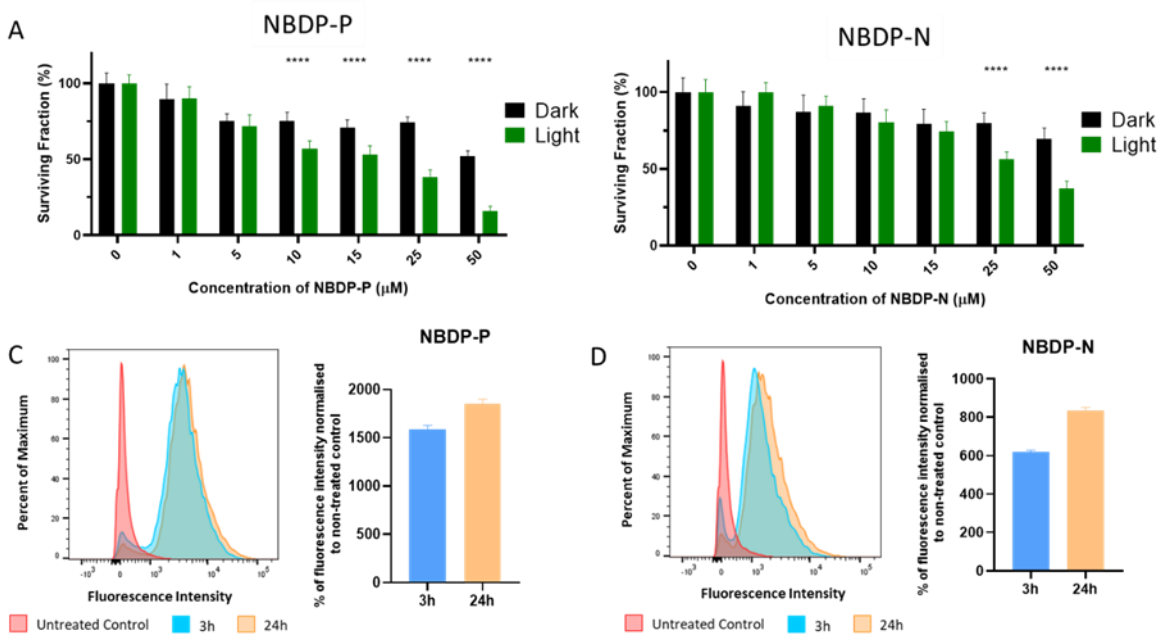

Figure 4. Biological assessment in PANC-1 cells. (**A**,**B**) Cell viability after PDT treatments with **NBDP-P** (**A**) or **NBDP-N** (**B**). Green bars show viability 48 h after illumination and black bars represent dark toxicity (non-illuminated group). Statistically significant differences are labeled as **** $P < 0.0001$ for comparisons between dark and photo-toxicity. (**C**,**D**) Internalization studies in cells incubated with **NBDP-P** (**C**) or **NBDP-N** (**D**). Histograms represent 20,000 cells analyzed per condition: untreated controls (red), 3 h incubation with the *N*-BODIPYs (blue) or 24 h incubation (orange). Fluorescence intensity was analyzed at 0 h post-incubation. Bar charts show median fluorescence intensity of the afore-mentioned incubation times normalized to untreated controls.

2.3.3. Subcellular Localization

The intense green fluorescence emission of both *N*-BODIPYs was visualized in PANC-1 cells after incubating the cells with the compounds for only 3 h (Figure 5). Morphological assessment of the fluorescence signal suggested that both compounds tend to localize within the mitochondria.

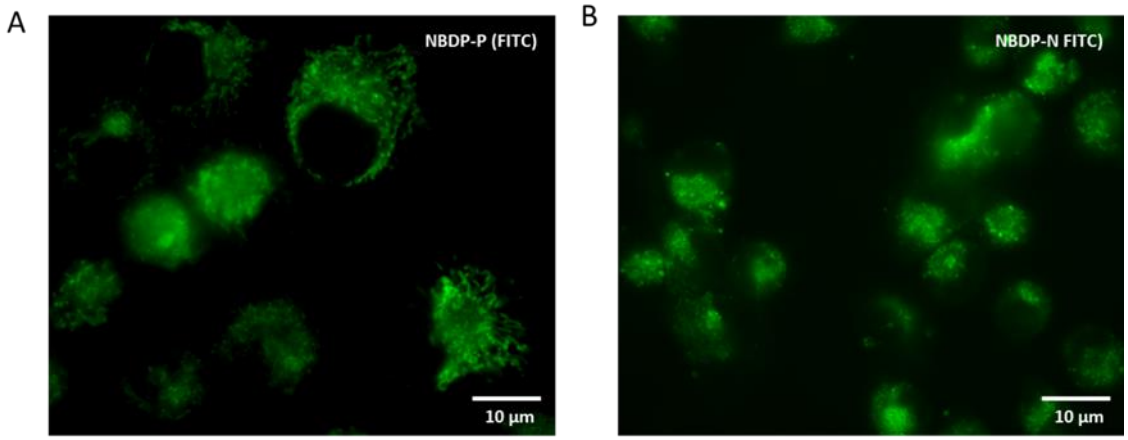

Figure 5. Live cell imaging of PANC-1 cells incubated with 5 μM of (**A**) **NBDP-P** or (**B**) **NBDP-N** for 3 h. The fluorescence pattern suggests a mitochondrial subcellular localization. Scale bar = 10 μm.

3. Materials and Methods

3.1. Synthetic Procedures

General. Common solvents were dried and distilled by standard procedures. All starting materials and reagents were obtained commercially and used without further purifications. Elution flash chromatography was conducted on silica gel (230 to 400 mesh ASTM). Thin layer chromatography (TLC) was performed on silica gel plates (silica gel 60 F254, supported on aluminum). The NMR spectra were recorded at 20 °C, and the residual solvent peaks were used as internal standards. The NMR signals are given in ppm. The DEPT-135 NMR experiments were used for the assignation of the type of carbon nucleus (C, CH, CH_2, and CH_3). The FTIR spectra were recorded from neat samples using ATR technique and IR bands are given in cm^{-1}.

4-{*N*-[2-(butylsulfonamido)ethyl]sulfamoyl}benzoic acid (**1**): A solution of 4-(chlorosulfonyl)benzoic acid (1.20 g, 5.5 mmol) in CH_2Cl_2 (2 mL) was dropwise added over a solution of *N*-(2-aminoethyl)butane-1-sulfonamide [25] (1.00 g, 5.5 mmol) and trimethylamine (0.56 g, 5.5 mmol) in CH_2Cl_2 (10 mL) under argon atmosphere at 0 °C. The reaction mixture was stirred overnight at room temperature. After reaction completion, 3M HCl (15 mL) was added and a white solid precipitated, which was filtered and washed, first, with diethyl ether (3 × 20 mL) and, then, with cold ethanol (3 × 20 mL). **1** (1.90 g, 95%) was obtained as a white solid. ^{1}H NMR (MeOH-d_4, 300 MHz) δ 8.95 (d, J = 8.4 Hz, 2H), 8.72 (d, J = 8.4 Hz, 2H), 7.89 (t, J = 6.0 Hz, 1H), 3.79–3.70 (m, 4H), 3.70–3.63 (m, 2H), 2.35 (m, 2H), 2.15 (sext, J = 7.5 Hz, 2H), 1.66 (t, J = 7.5 Hz, 3H) ppm.

Propargyl 4-{*N*-[2-(butylsulfonamido)ethyl]sulfamoyl}benzoate (**2**): A mixture of **1** (1.00 g, 2.74 mmol), *N*-[3-(dimethylamino)propyl]-*N*′-ethylcarbodiimide hydrochloride (526 mg, 2.74 mmol), 4-(dimethylamino)pyridine (670 mg, 5.48 mmol) and propargyl alcohol (154 mg, 2.74 mmol) in CH_2Cl_2 (5mL) was stirred at room temperature for 24 h under argon atmosphere. After reaction completion, water (15 mL) and CH_2Cl_2 (15 mL) were added, the phases were separated, and the aqueous phase was extracted with CH_2Cl_2 (3 × 15 mL). The organic phase was successively washed with 3 M HCl (1 × 15 mL), water (1 × 15 mL), 10% aqueous NaOH (1 × 15 mL), water (1 × 15 mL) and brine (1 × 15 mL). The organic phase was dried over anhydrous Na_2SO_4, filtered and the solvent was removed under reduced pressure. The obtained residue was purified by flash chromatography (silica gel, hexane/ethyl acetate, 1:1) to obtain **2** (1.10 g, 99%) as a white solid. ^{1}H NMR ($CDCl_3$, 300 MHz) δ 8.18 (d, J = 8.5 Hz, 2H), 7.95 (d, J = 8.5 Hz, 2H), 5.85 (t, J = 6.0 Hz, 1H), 5.27 (t, J = 6.1 Hz, 1H), 4.95 (d, J = 2.5 Hz, 2H), 3.33–3.20 (m, 2H), 3.18–3.08 (m, 2H), 3.03 (m, 2H), 2.55 (t, J = 2.4 Hz, 1H), 1.75 (m, 2H), 1.43 (sext, J = 7.4 Hz, 2H), 0.92 (t, J = 7.3 Hz, 3H) ppm. ^{13}C NMR ($CDCl_3$, 75 MHz) δ 164.5 (C), 144.1 (C), 133.4 (C), 130.8 (CH), 127.3 (CH), 77.3 (C), 75.7 (CH), 53.2 (CH_2), 52.8 (CH_2), 43.8 (CH_2), 43.2 (CH_2), 25.6 (CH_2), 21.6 (CH_2), 13.7 (CH_3) ppm. FTIR ν 3281, 1729, 1326, 1270, 1164, 1142 cm^{-1}.

NBDP-yne: BCl_3 (1M in hexanes, 0.3 mL, 0.30 mmol) was dropwise added over a solution of 2,6-diethyl-1,3,5,7,8-pentamethyl-*F*-BODIPY (PM567; 50 mg, 0.16 mmol) in dry CH_2Cl_2 (5 mL) under argon atmosphere. The reaction mixture was stirred for 5 min (disappearance of starting *F*-BODIPY was monitored by TLC). Then, triethylamine (127 mg, 1.26 mmol) was added, followed by **2** (190 mg, 0.47 mmol) and the reaction mixture was stirred for 30 min at rt. The reaction mixture was filtered through celite®, washed with CH_2Cl_2 and the solvent evaporated under reduced pressure. The obtained residue was purified by flash chromatography (silica gel, hexane/ethyl acetate, 6:4) to obtain **NBDP-yne** (77 mg, 72%) as an orange solid. ^{1}H NMR ($CDCl_3$, 300 MHz) δ 7.98 (d, J = 8.5 Hz, 2H), 7.42 (d, J = 8.2 Hz, 2H), 4.95 (d, J = 2.5 Hz, 2H), 3.72–3.60 (m, 4H), 2.70 (s, 3H), 2.55 (t, J = 2.4 Hz, 1H), 2.47 (m, 2H), 2.38 and 2.31 (ABX_3 system, AB section, J_{AB} = 15.0 Hz, $J_{AX} = J_{BX}$ = 7.5 Hz, 4H), 2.39 (s, 6H), 2.05 (s, 6H), 1.58–1.51 (m, 2H), 1.23 (sext, J = 7.4 Hz, 2H), 1.01 (ABX_3 system, X_3 section, $J_{AX} = J_{BX}$ = 7.5 Hz, 6H), 0.79 (t, J = 7.4 Hz, 3H) ppm. ^{13}C NMR ($CDCl_3$, 75 MHz) δ 164.7 (C), 151.0 (C), 144.3 (C), 140.4 (C), 137.2 (C), 133.3 (C), 133.1 (C), 132.1 (C), 130.1 (CH), 127.0 (CH), 75.6 (CH), 53.1 (CH_2), 51.1 (CH_2), 45.1 (CH_2), 44.6 (CH_2), 24.7 (CH_2), 21.9 (CH_2), 17.9 (CH_3), 17.4 (CH_2), 15.1 (CH_3), 13.6 (CH_3), 12.7 (CH_3) ppm. ^{11}B NMR ($CDCl_3$, 160 MHz) δ −1.08 (s) ppm. FTIR ν 1730, 1563, 1480, 1329, 1195 cm^{-1}.

NBDP-N: *Click reaction:* Over a mixture of **NBDP-yne** (25 mg, 0.037 mmol) and 3-azido-*N*,*N*-dimethylpropanamine [26] (6 mg, 0.044 mmol) in 2 mL of *t*-BuOH, $CuSO_4 \cdot 5H_2O$ (4 mg, 0.015 mmol)

in water (1 mL) and, then, sodium ascorbate (6 mg, 0.030 mmol) in water (1 mL) were dropwise added. The reaction mixture was stirred for 24 h at room temperature. After reaction completion, water (15 mL) and CH_2Cl_2 (15 mL) were added, the phases were separated and the aqueous phase was extracted with CH_2Cl_2 (3 × 15 mL), dried over Na_2SO_4, filtered and the solvent was evaporated under reduced pressure. *Amine quaternization:* The reaction crude (25 mg, 0.031 mmol) was dissolved in CH_2Cl_2 (2 mL) and iodomethane (1.14 g, 8.0 mmol) was dropwise added. The reaction mixture was stirred for 30 min. Then, diethyl ether (2 mL) was added and an orange solid precipitated. The precipitate was filtered and washed with diethyl ether (30 mL). The precipitate was redissolved in CH_2Cl_2 and the solvent was removed under reduced pressure. **NBDP-N** (58 mg, 96%) was obtained as a reddish orange solid. ^{1}H NMR ($CDCl_3$, 300 MHz) δ 8.13 (s, 1H), 7.96 (d, J = 8.5 Hz, 2H), 7.37 (d, J = 8.3 Hz, 2H), 5.44 (s, 2H), 4.60 (t, J = 6.8 Hz, 2H), 3.82 (m, 2H), 3.66 (m, 4H), 3.33 (s, 9H), 2.68 (s, 3H), 2.56 (m, 2H), 2.46 (m, 2H), 2.47–2.20 (m, 4H), 2.38 (s, 6H), 2.02 (s, 6H), 1.87 (br. s, 2H), 1.51 (m, 2H), 1.21 (sext, J = 7.4 Hz, 2H), 0.97 (t, J = 7.5 Hz, 6H), 0.77 (t, J = 7.3 Hz, 3H) ppm. ^{13}C NMR ($CDCl_3$, 75 MHz) δ 165.1 (C), 150.9 (C), 144.0 (C), 142.7 (C), 140.5 (C), 137.2 (C), 133.3 (C), 133.1 (C), 132.5 (C), 130.2 (CH), 126.9 (CH), 125.4 (CH), 63.8 (CH_2), 58.7 (CH_2), 54.2 (CH_3), 51.0 (CH_2), 46.7 (CH_2), 45.1 (CH_2), 44.6 (CH_2), 24.6 (CH_2), 24.3 (CH_2), 21.8 (CH_2), 17.9 (CH_3), 17.3 (CH_2), 15.2 (CH_3), 15.2 (CH_3), 13.5 (CH_3), 12.7 (CH_3) ppm. ^{11}B NMR ($CDCl_3$, 160 MHz) δ–1.09 (s) ppm. FTIR ν 1721, 1563, 1477, 1321, 1270, 1194, 1014 cm^{-1}.

NBDP-P: Following the procedure described above for the *click* reaction in the synthesis of **NBDP-N**, $CuSO_4 \cdot 5H_2O$ (4 mg, 0.015 mmol), sodium ascorbate (6 mg, 0.030 mmol), **NBDP-yne** (25 mg, 0.037 mmol) and (3-azidopropyl)triphenylphosphonium bromide [27] (19 mg, 0.044 mmol) were reacted. After purification by flash chromatography (silica gel, CH_2Cl_2/MeOH, 9:1), **NBDP-P** (34 mg, 84%) was obtained as a red solid. ^{1}H NMR ($CDCl_3$, 300 MHz) δ 8.47 (br. s, 1H), 7.93 (d, J = 2H), 7.82–7.60 (m, 15H), 7.35 (d, J = 2H), 5.46 (s, 2H), 5.00 (m, 2H), 3.85 (m, 2H), 3.67 (m, 4H), 2.68 (s, 3H), 2.46 (m, 2H), 2.41–2.19 (m, 6H), 2.37 (s, 6H), 2.03 (s, 6H), 1.52 (m, 2H), 1.21 (sext, J = 7.3 Hz, 2H), 0.97 (t, J = 7.5 Hz, 6H), 0.77 (t, J = 7.3 Hz, 3H) ppm. ^{13}C NMR ($CDCl_3$, 75 MHz) δ 165.1 (C), 151.0 (C), 143.9 (C), 142.1 (C), 140.4 (C), 137.1 (C), 135.4 (d, $J_{13C\text{-}31P}$ = 3.1 Hz, CH), 133.7 (d, $J_{13C\text{-}31P}$ = 10.1 Hz, CH), 133.3 (C), 133.1 (C), 132.6 (C), 130.8 (CH), 130.7 (CH), 130.1 (CH), 126.9 (CH), 126.7 (CH), 117.7 (d, $J_{13C\text{-}31P}$ = 86.5 Hz, C), 117.2 (C), 58.6 (CH_2), 51.1 (CH_2), 49.3 (d, $J_{13C\text{-}31P}$ = 18.8 Hz CH_2), 45.1 (CH_2), 44.5 (CH_2), 24.6 (CH_2), 23.5 (CH_2), 21.8 (CH_2), 20.0 (d, $J_{13C\text{-}31P}$ = 59.9 Hz, CH_2), 17.8 (CH_3), 17.3 (CH_2), 15.1 (CH_3), 13.5 (CH_3), 12.7 (CH_3) ppm. ^{11}B NMR ($CDCl_3$, 160 MHz) δ −1.09 (s) ppm. ^{31}P NMR ($CDCl_3$, 121 MHz) δ 27.2 (s) ppm. FTIR ν 1721, 1563, 1477, 1326, 1270, 1193, 1053, 980 cm^{-1}.

3.2. Photophysical Properties

Diluted solutions of **NBDP-yne** (around 2 × 10^{-6} M) were prepared by adding the corresponding solvent (spectroscopic grade) to the residue from the adequate amount of a concentrated stock solution in acetone, after vacuum evaporation of this solvent. The cationic **NBDP-N** and **NBDP-P** were directly dissolved in methanol and diluted to reach the required micromolar concentration. UV-Vis absorption and steady-state fluorescence were recorded on a Varian model CARY 4E spectrophotometer and an Edinburgh Instruments spectrofluorimeter (model FLSP920), respectively, using 1 cm path length quartz cuvettes. The emission spectra were corrected from the monochromator wavelength dependence, the lamp profile and the photomultiplier sensitivity. Fluorescence quantum yields (ϕ) were calculated using commercial PM567 (ϕ^r = 0.84 in ethanol) as reference. The values were corrected by the refractive index of the solvent. Radiative decay curves were registered with the time correlated single-photon counting technique (Edinburgh Instruments, model FL920, with picosecond time-resolution). Fluorescence emission was monitored at the maximum emission wavelength after excitation at 470 nm by means of a diode laser (PicoQuant, model LDH470, respectively) with 150 ps full width at half maximum (FWHM) pulses. The fluorescence lifetime (τ) was obtained after the deconvolution of the instrumental response signal from the recorded decay curves by means of an iterative method. The goodness of the exponential fit was controlled by statistical parameters (chi-square and the analysis of the residuals).

3.3. Biological Assessment

3.3.1. Cell culture

Human pancreatic ductal adenocarcinoma (PANC-1) cells were purchased from the American Type Culture Collection (ATCC® CRL-1469™) and grown as monolayer cultures in Dulbecco's Modified Eagle's Medium (DMEM; Sigma-Aldrich, St Louis, MA, USA) supplemented with 10% (*v*/*v*) fetal bovine serum (FBS), 50 U/mL penicillin and 50 mg/mL streptomycin. All products were purchased from Gibco (Paisley, UK). Cell cultures were performed in a 5% CO_2 atmosphere plus 95% air at 37 °C, and maintained in 75 cm^2 tissue culture flasks (TPP, Switzerland) in a BINDER incubator (Tuttlingen, Germany). Depending on the experiment, cells were seeded in 96-well plates, 6-well plates (TPP), or in 24-well plates with 10 mm square glass coverslips. Sub-confluent cell cultures were used.

3.3.2. Photodynamic Therapy Treatments

For testing the suitability of **NBDP-P** and **NBDP-N** as photosensitizers for PDT, 5×10^3 cells/well were seeded on 96-well plates. After 24 h, cells were incubated with increasing concentrations of *N*-BODIPYs (1–50 μM) for 24 h. Then, cells were washed with PBS and maintained in DMEM during irradiation and post-treatment time (48 h). Illumination was performed by means of a green light-emitting diode (LED) device (λ = 525 nm) with a fluence rate of 5.73 mW/cm^2, measured with an M8 Spectrum Power Energy meter (Merchantek Inc., San Diego, CA, USA). The total light dose used was 10.3 J/cm^2. Simultaneous experiments were carried out by incubation with the corresponding *N*-BODIPYs but without irradiation (dark toxicity), in order to analyze a possible cytotoxic effect induced by the dyes.

3.3.3. Cell Viability Studies

Dark and photo-toxicity induced effects on PANC-1 cells were measured by the dimethylthiazolyl-diphenyl-tetrazolium bromide (MTT; Sigma-Aldrich) colorimetric assay. Briefly, 100 μL/well of a 0.5 mg/mL MTT solution were added to each well following PDT treatments (or alternatively dark conditions). After 1 h incubation, the reduced formazan was dissolved using 100 μL/well dimethylsulfoxide and absorbance (optical density, OD) was measured at 562 nm using an Infinite M200 PRO microplate reader (Tecan Group Ltd.). Cell viability was calculated as the percentage of OD of treated cells compared to untreated (control) cells. Data is shown as mean values ± standard deviation from at least three different experiments. For statistical calculations one-way ANOVA Tukey's test and the software GraphPad Prism 7.03 (GraphPad Software, La Jolla, CA, USA) were used. *P*-values < 0.0001 (****) were considered as statistically significant.

3.3.4. N-BODIPY Cellular Uptake by Flow Cytometry

To evaluate the cell internalization of *N*-BODIPYs, PANC-1 cells were seeded on 6-well plates at a density of 5×10^5 cells/well. After 24 h, cells were incubated with 1 μM **NBDP-P** or **NBDP-N** for 3 or 24 h. Then, cells were washed 3 times with PBS, harvested using trypsin-EDTA (Gibco), and centrifuged at 13,200 rpm for 10 s. After that, cells were re-suspended in PBS. Fluorescence intensity was measured using a BD LSRII™ cell analyzer (BD Bioscience, UK) with a laser line at 488 nm (green) and complemented with appropriate filters. A total of 20,000 events/sample were recorded and single cells were discriminated from doublets by pulse-processing. FlowJo v10 software (Tree Star, Inc, USA) was used to analyze and plot the acquired data.

3.3.5. Subcellular Localization and Accumulation by Fluorescence Microscopy

To study the subcellular localization of *N*-BODIPYs, 5×10^4 cells were seeded on glass coverslips placed on 24-well plates. Cells were incubated with 5 μM of *N*-BODIPY **NBDP-P** or **NBDP-N** for 3 h and washed three times with PBS prior to visualization. An Olympus BX63 microscope equipped

with an Olympus DP80 digital camera (Olympus, USA) was used for these experiments. A FITC filter (490–520 nm) was used to excite both *N*-BODIPYs.

4. Conclusions

A key intermediate for the multifunctionalization of BODIPYs towards biophotonics has been designed and obtained. This intermediate is based on an *N*-BODIPY having an alkynyl moiety that has been easily derivatized using *click chemistry* to obtain two BODIPY dyes for the labelling of mitochondria. The functionalization through the boron atom helps the new dyes keep the photophysical properties of parent *F*-BODIPY. Additionally, the promising MTT data obtained, together with the fast internalization and mitochondria-labelling of **NBDP-P** and **NBDP-N** in PANC-1 cells, given the great importance that mitochondria play in cancer cells (regulating key functions such as ATP generation, redox homeostasis, metabolic signaling and control of apoptotic pathways), indicate the potential of **NBDP-P** and **NBDP-N** as starting platforms for the development of smarter photosensitizers for PDT.

Author Contributions: Conceptualization, S.d.l.M., B.L.M., P.A. and A.V.; methodology, B.L.M.; J.B., P.A. and A.V.; validation, P.A., M.J.O. and B.L.M.; formal analysis, F.M., J.B., A.G.-S., P.A. and A.V.; investigation, C.R., C.S., A.G.-S. and E.A.-Z.; writing—original draft preparation, B.L.M., J.B. and P.A.; writing—review and editing, S.d.l.M., A.G.-S. and A.V.; supervision, J.B., S.d.l.M., P.A. and A.V.; project administration, S.d.l.M., M.J.O., J.B., A.V. and P.A.; funding acquisition, S.d.l.M., M.J.O., J.B. and P.A. All authors have read and agreed to the published version of the manuscript.

Funding: This research was funded by the Spanish MICIU, grant number MAT201783856-C3-2-P and -3-P; by Gobierno Vasco, grant number IT912-16 and by the Spanish Ministerio de Economía y Competitividad (MINECO), grant number CTQ2016-78454-C2-2-R. C.R. and C.S. thank Comunidad de Madrid/UCM for a research contract. E.A.-Z. thanks Gobierno Vasco for a predoctoral fellowship. P.A. thanks the Ramón Areces Foundation for a Postdoctoral fellowship. P.A. is supported by a Biomedical Research Centre-UCLH Charities Fast Track Grant.

Conflicts of Interest: The authors declare no conflict of interest.

References

1. Prasad, P.N. *Introduction to Biophotonics*; Wiley-Interscience: New York, NY, USA, 2003.
2. Lovell, J.F.; Liu, T.W.B.; Chen, J.; Zheng, G. Activatable photosensitizers for imaging and therapy. *Chem. Rev.* **2010**, *110*, 2839–2857, doi:10.1021/cr900236h.
3. van Straten, D.; Mashayekhi, V.; de Bruijn, H.S.; Oliveira, S.; Robinson, D.J. Oncologic Photodynamic Therapy: Basic Principles, Current Clinical Status and Future Directions. *Cancers* **2017**, *9*, 19, (54 pages), doi:10.3390/cancers9020019.
4. Hambling, M.R.; Huang, Y. *Imaging in Photodynamic Therapy (Series in Cellular and Clinical Imaging)*; CRC Press: Boca Raton, FL, 2017.
5. Ferreira dos Santos, A.; Quieroz de Almeida, D.R.; Ferreira Terra, L.; Baptista, M.S.; Labriola, L. Photodynamic therapy in cancer treatment—An update review. *J. Cancer Metastasis Treat* **2019**, *5*, 25 (20 pages), doi:10.3322/caac.20114.
6. Acedo, P.; Stockert, J.C.; Cañete, M.; Villanueva, A. Two combined photosensitizers: A goal for more effective photodynamic therapy of cancer. *Cell Death Dis.* **2014**, *5*, e1122, doi:10.1038/cddis.2014.77.
7. Xiaoyuan, C.; Stephen, W. *Cancer Theranostics*; Elsevier: Amsterdam, The Netherlands, 2014.
8. Li, B.; Zhao, M.; Zhang, F. Rational Design of Near-Infrared-II Organic Molecular Dyes for Bioimaging and Biosensing. *ACS Mater. Lett.* **2020**, *2*, 905–917, doi:10.1021/acsmaterialslett.0c00157.
9. Kowada, T.; Maeda, H.; Kikuchi, K. BODIPY-based probes for the fluorescence imaging of biomolecules in living cells. *Chem. Soc. Rev.* **2015**, *44*, 4953–4972, doi:10.1039/C5CS00030K.
10. Kamkaew, A.; Lim, S.H.; Lee, H.B.; Kiew, L.V.; Chung, L.Y.; Burgess, K. BODIPY dyes in photodynamic therapy. *Chem. Soc. Rev.* **2013**, *42*, 77–88, doi:10.1039/C2CS35216H.
11. Prieto-Montero, R.; Prieto-Castañeda, A.; Sola-Llano, R.; Agarrabeitia, A.R.; García-Fresnadillo, D.; López-Arbeloa, I.; Villanueva, A.; Ortiz, M.J.; de la Moya, S.; Martínez-Martínez, V. Exploring BODIPY Derivatives as Singlet Oxygen Photosensitizers for PDT. *Photochem. Photobiol.* **2020**, *96*, 458–477, doi:10.1111/php.13232.

12. Bañuelos, J. BODIPY Dye, the Most Versatile Fluorophore Ever? *Chem. Rec.* **2016**, *16*, 335–348, doi:10.1002/tcr.201500238.
13. Loudet, A.; Burgess, K. BODIPY Dyes and Their Derivatives: Syntheses and Spectroscopic Properties. *Chem. Rev.* **2007**, *107*, 4891–4932, doi:10.1021/cr078381n.
14. Clarke, R.G.; Hall, M.J. Chapter Three—Recent developments in the synthesis of the BODIPY dyes. In *Advances in Heterocyclic Chemistry*; Hall, M.J., Ed.; Academic Press: Cambridge, MA, USA, 2019; Volume 128, pp. 181–261.
15. Zhao, J.; Xu, K.; Yang, W.; Wang, Z.; Zhong, F. The triplet excited state of Bodipy: Formation, modulation and application. *Chem. Soc. Rev.* **2015**, *44*, 8904–8939, doi:10.1039/c5cs00364d.
16. Alamudi, S.H.; Satapathy, R.; Kim, J.; Su, D.; Ren, H.; Das, R.; Hu, L.; Alvarado-Martínez, E.; Lee, J.Y.; Hoppmann, C.; et al. Development of background-free tame fluorescent probes for intracellular live cell imaging. *Nat. Commun.* **2016**, *7*, 11964, doi:10.1038/ncomms11964.
17. Fan, G.; Yang, L.; Chen, Z. Water-soluble BODIPY and aza-BODIPY dyes: Synthetic progress and applications. *Front. Chem. Sci. Eng.* **2014**, *8*, 405–417, doi:10.1007/s11705-014-1445-7.
18. Bodio, E.; Goze, C. Investigation of B-F substitution on BODIPY and aza-BODIPY dyes: Development of B-O and B-C BODIPYs. *Dyes Pigments* **2019**, *160*, 700–710, doi:10.1016/j.dyepig.2018.08.062.
19. Ray, C.; Díaz-Casado, L.; Avellanal-Zaballa, E.; Bañuelos, J.; Cerdán, L.; García-Moreno, I.; Moreno, F.; Maroto, B.L.; López-Arbeloa, Í.; de la Moya, S. *N*-BODIPYs Come into Play: Smart Dyes for Photonic Materials. *Chem. Eur. J.* **2017**, *23*, 9383–9390, doi:10.1002/chem.201701350.
20. Kim, E.; Koo, H. Biomedical applications of copper-free click chemistry: In vitro, in vivo, and ex vivo. *Chem. Sci.* **2019**, *10*, 7835–7851.
21. Gao, T.; He, H.; Huang, R.; Zheng, M.; Wang, F.-F.; Hu, Y.-J.; Jiang, F.-L.; Liu, Y. BODIPY-based fluorescent probes for mitochondria-targeted cell imaging with superior brightness, low cytotoxicity and high photostability. *Dyes Pigments* **2017**, *141*, 530–535, doi:10.1016/j.dyepig.2017.03.009.
22. Alamudi, S.H.; Chang, Y.-T. Advances in the design of cell-permeable fluorescent probes for applications in live cell imaging. *Chem. Commun.* **2018**, *54*, 13641–13653, doi:10.1039/C8CC08107G.
23. Lee, M.H.; Han, J.H.; Lee, J.-H.; Choi, H.G.; Kang, C.; Kim, J.S. Mitochondrial Thioredoxin-Responding Off-On Fluorescent Probe. *J. Am. Chem. Soc.* **2012**, *134*, 17314–17319, doi:10.1021/ja308446y.
24. Robinson, K.M.; Janes, M.S.; Pehar, M.; Monette, J.S.; Ross, M.F.; Hagen, T.M.; Murphy, M.P.; Beckman, J.S., Selective fluorescent imaging of superoxide in vivo using ethidium-based probes. *Proc. Natl. Acad. Sci. USA* **2006**, *103*, 15038–15043, doi:10.1073/pnas.0601945103.
25. St John-Campbell, S.; White, A.J.P.; Bull, J.A. Single Operation Palladium Catalysed C(sp3)-H Functionalisation of Tertiary Aldehydes: Investigations into Transient Imine Directing Groups. *Chem. Sci.* **2017**, *8*, 4840–4847, doi:10.1039/C7SC01218G.
26. Dash, J.; Waller, Z.A.E.; Pantoş, G.D.; Balasubramanian, S. Synthesis and Binding Studies of Novel Diethynyl-Pyridine Amides with Genomic Promoter DNA G-Quadruplexes. *Chem. Eur. J.* **2011**, *17*, 4571–4581, doi:10.1002/chem.201003157.
27. Knight, J.D.; Sauer, S.J.; Coltart, D.M. Asymmetric Total Synthesis of the Antimalarial Drug (+)-Mefloquine Hydrochloride via Chiral N-Amino Cyclic Carbamate Hydrazones. *Org. Lett.* **2011**, *13*, 3118–3121, doi:10.1021/ol2010193.